THE EFFECT OF FAR VORTEX WAKE ON INSTANTANEOUS INDUCED VELOCITIES IN THE PLANE OF ROTOR DISK AND IN ROTOR WAKE

Ruslan M.Mirgazov., Valentina M.Shcheglova

Central Aerodynamic Institute (TsAGI)
Zhukovsky Str., Zhukovsky, Moskow reg., 140160, Russian Federation
e-mail: xxx@tsagi.ru

Key words: rotor, vortex wake, far wake, induced velocity

Abstract: A combined efficient method is suggested to determine vortex sheet shape and induced velocities both in the disk plane and within vortex sheet for horizontal fight conditions. It includes determination of induced velocities from nonlinear vortex wakes of nv extent of deformed wake spiral turns (nv – a number of turns) with further addition of far vortex wake velocities computed using the disk theory.

Computations are made for flight conditions $\mu = 0.31$ and $\mu = 0.0917$. Computational results of induced velocities for different nonlinear vortex wake extent are compared with induced velocities determined by the combined method.

Evaluation of lateral vortex effect on induced velocities has been performed.

INTRODUCTION

Computation practice shows [1,2] that to obtain more reliable results when determining instantaneous induced velocities in disk plane, time-average induced velocities in rotor vortex wake as well as the wake shape it is necessary to take into consideration the extent of shedding from the blade vortices with nv = 30-40 and more turns, and the lesser the value of μ the greater number of turns defining the wake length is needed.
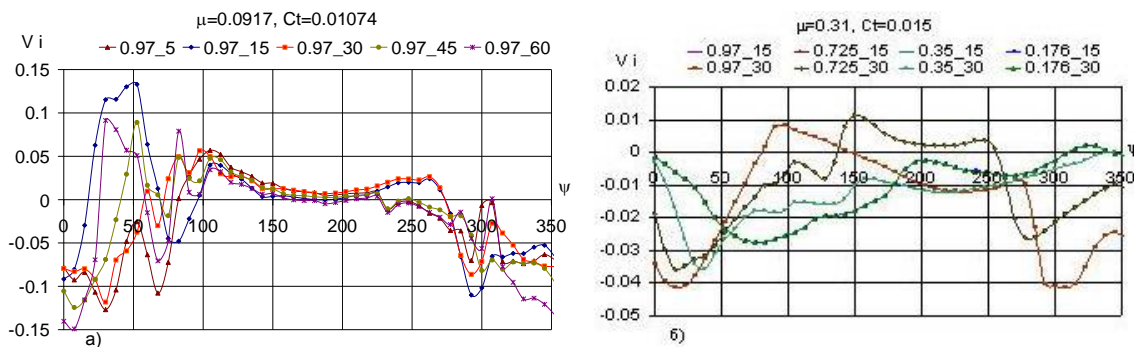
Figure 1: Distribution of induced velocities versus azimuth for values of nv = 5, 15, 30, 45 and 60 for one of the blade tip sections r/R=0.97 at $\mu = 0.0917$ (a) and at $\mu = 0.31$ (b)

The different number of vortex wake spiral turns was regarded both when calculating induced velocities and when correcting wake geometry with account of its nonlinear movements.

The wake geometry has an effect on instantaneous induced velocities (Fig.1a) which also considerably differ from one another at various nv values from nv = 5 to nv = 45 of vortex spiral turns at flight conditions μ = 0.0917 (the circulation is given). The tendency for rapid convergence of velocity values is not observed, i.e. it is difficult to say anything of the required vortex wake length. Computations show that at low values of μ (not only for μ = 0.0917) the taken number of vortex wake turns is evidently not enough to obtain more reliable results. At Fig.1b the computational results at flight conditions of μ = 0.31 are presented for the blades with given intensities of vortices of different vortex wake length. As is seen from plots the vortex wake length has no effect on instantaneous induced velocities at flight conditions μ = 0.31. All computations can be made at wake length, for example, of 5 turns (shortened wake). More detailed computations for this regime including the circulation determined from combined computation of loads and induced velocities in view of the far wake were not performed.

The need for taking into account the far wake effect is also illustrated by data in Table 1. In this Table average induced disk velocities are presented against the rotor vortex wake length (nv) as well as the average induced velocity regarding the extended wake as compared to the average induced velocity which is specified at the beginning of vortex sheet shape computation.

Table I

Computation at given circulation

μ=0.0917			
nv	Viрасч	Viзад	%
5	-0.02947	-0.02808	4.95
15	-0.03445	-0.02808	22.75
30	-0.02641	-0.02808	5.96
45	-0.03035	-0.02808	8.11
∞	-0.02758	-0.02808	1.79

μ=0.31			
nv	Viрасч	Viзад	%
5	-0.01125	-0.01164	3.35
15	-0.01125	-0.01164	3.35
30	-0.01125	-0.01164	3.35

Computation at determined circulation

μ=0.0917			
nv	Viрасч	Viзад	%
5	-0.029	-0.0268	7.58
15	-0.025	-0.0268	6.71
∞	-0.02626	-0.0268	2.015

From data presented in Table 1 it follows that computation by the combined method may reduce the error rate. Similar investigation was conducted in paper [2] for one of the transient values of μ = 0.195 where it was also shown that including of the far wake effect is important.

Taking account of the extent of shedding vortices having 30-45 turns requires profound computation procedures and consequently much time for computations which is not suitable for average-power computers. This suggests that the computational model should be simplified for algorithm practical realization using computers of this kind. For this purpose, a combined computational method using the disk theory is suggested allowing for considerable reduction of time required for computations.

1. FORMULATION OF THE PROBLEM

A combined method for calculating the induced velocities in the rotor disk plane and in rotor vortex wake includes determination of induced velocities from nonlinear vortex wakes of small extent (nv = 5, for example) with further addition of induced velocities from the far vortex wakes computed using the disk theory. The main ideas of the method for determination of wake shapes and induced velocities are presented in paper [1] where for oblique flow a relatively efficient method is suggested to determine vortex shapes and induced velocities both in rotor plane and in its vortex wake using nonlinear model.

For viscid fluid the induced velocity at any point of space can be found by the relationship [1,3]

$$\upsilon = \int_L \frac{\overline{\Gamma}}{4\pi} \cdot \frac{d\vec{l} \times \vec{r}}{r^3} \cdot K(r),$$ (1.1)

where $\vec{r}$ is a vector connecting $d\vec{l}$ element to velocity computation point, a factor K(r) provides for vortex distribution within the core under the diffusion for which approximation by function [1] $K(r) = \dfrac{r^2}{(r^2 + \varepsilon^2)^{3/2}}$ is appropriate to speed up the calculation process. Here $\varepsilon = 1/2 \cdot \delta$ is a positive small value ($\delta = 2\sqrt{vt}$), v is a kinematic viscosity coefficient, where t is a diffusion time.

Vortex element transport is defined by the following equation

$$\frac{d\vec{r}(s,\tau,t)}{dt} = \vec{\upsilon} + \vec{V}_0,$$ (1.2)

at the initial condition $\vec{r}(s,\tau,t)_{t=\tau} = \vec{r}_0(s,\tau)$. Here s are coordinates of points position, t is a considered instant of time, τ is a moment of shedding of vortex element (time of diffusion is estimated from time instant τ), $\vec{V}_0$ is an incoming flow in horizontal flight which makes an effective angle of attack $\alpha_{ef} = \alpha_c + a_1$ with rotor disk plane where α_c is a constructive rotor angle of attack, a_1 is an angle of rotor axis tilt in the xoy plane at flapping motion.

The method is based on vortex sheet representation in wind-axes coordinate system and consequent account for deformations at points of a series of "sections" perpendicular to the incoming flow velocity. The movement of computational points in one such "section" has little effect on the velocities in the other such "section" resulting in rapid convergence of successive approximations. The refinement of coordinates of nonlinear vortex system shape (1.2) is performed using the first-order Euler's formulas in time. In this case in order to save calculation time the refinements obtained at each step are used only at subsequent steps, i.e. the refinements in "sections" lying after the calculated section at the given step are not

introduced. In "sections" lying before the calculated section the coordinates are corrected by the increments in calculated section as compared to the previous increment. The given algorithm is distinguished from other algorithms by the fact that a comprehensive account for radius and azimuth circulation variations requires a moderate number of computational operations.

Vortices shedding from blade at points ($\bar{r}$, ψ) shift with constant drift velocity $\vec{V}_0$ and make with longitudinal axis x an angle α_c equal to

$$\alpha_c = \arcsin\left(\frac{\overline{V_y}}{\overline{\overline{V_y}}}\right), \tag{1.3}$$

where $\overline{V_x}$ and $\overline{V_y}$ are the incoming flow velocity projections on the axes ox and oy corresponding to the equations $\overline{V_y} = (-\overline{V_0} \cdot \sin\alpha_э - \overline{V_i}) \cdot \cos\alpha_э$, $\overline{V_x} = \overline{V_0} - (-\overline{V_0} \cdot \sin\alpha_э - \overline{V_i}) \cdot \sin\alpha_э$, where $\overline{V_i} = -\dfrac{C_t}{(0.313 \cdot 12 \cdot \overline{V_0})}$ is an average axis component of disk induced velocity which can be approximately determined from this relationship.

Values of shedding vortex circulation can be specified by preliminary computations or defined in the process of combined calculation of rotor aerodynamic loads and vortex sheet shape and induced velocities. Within the scope of blade nonlinear theory the rotor is replaced by lifting vortex lines with variable azimuth and radius circulation $\overline{\Gamma}(\bar{\rho}, \psi) = \Gamma(\bar{\rho}, \psi)/(\omega R^2)$ and circulation of free longitudinal and lateral vortices shedding from the blade sections equal to $\dfrac{\partial}{\partial\rho}\overline{\Gamma}(\bar{\rho}, \vartheta)\partial\rho$ and $\dfrac{\partial}{\partial\vartheta}\overline{\Gamma}(\bar{\rho}, \vartheta)\partial\vartheta$, respectively.

Solution of equations (1.2) is performed in discrete form. Taking a number of values of discrete points $\rho = \rho_j$, $\vartheta = \vartheta_i$, $\psi = \psi_p$ the vortex sheet is replaced by the grid consisting of straight-line segments of vortex filaments. The results of the program realizing this algorithm are presented in Fig. 2 where the shape of nonlinear vortex wake at wake segment with free vortex extent nv = 5 turns is presented in two projections.

The last computational points of this wake which belong to vortices consisting of a set of $K_L \cdot \psi$ vortex sheets, have coordinates x_j, y_j, z_j through

Figure 2: $\mu=0{,}0917$. Shape of rotor vortex wake from tip vortices of each blade in two spiral projections at $\mu=0{,}0917$

4

which a set of curves $Li_j(\psi, K_L, x_j, y_j, z_j)$ goes, where ψ - is a blade azimuth at rotor rotation, j – is blade span computational points number, K_L - a number of rotor blades. Vortices going from points with above mentioned coordinates lying on curves Li_j generate a wake in the form of semi-infinite cylinder having straight generating lines and a known intensity. This wake is termed as a far wake. From these far vortices using the disk theory additions to instantaneous induced velocities obtained by nonlinear theory for a shortened 5-turn wake are determined over the blade span.

The curves Li_j are nothing but the last "section" deformed during computation in which vortices of the far wake (Figs. 3 and 4) are seated against at points with coordinates x_j, y_j z_j. The above cylinder formed by rectilinear vortices is directed along drifting line, determined by the angle α_d (1.3).
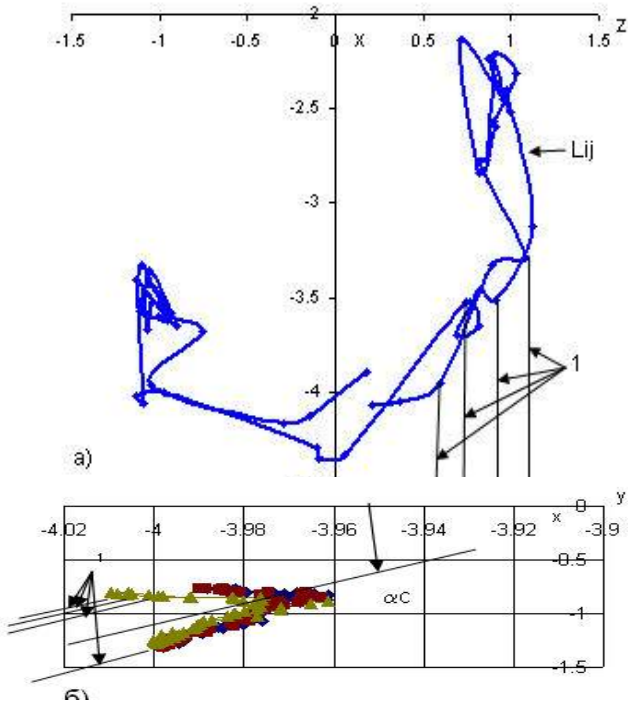
Figure 3: Diagram of far longitudinal and lateral vortices location: a) – frontal projection, b) – transversal projection, 1 –longitudinal vortices

The frontal projection of the last "section" at the final moment of wake formation is presented in Figs. 3a and 4. For linear vortex system the projection would represent an ellipse. For nonlinear vortex system the specified ellipse is badly deformed creating complicated intersecting contours with bends that appear on the plan ellipse curve (Fig. 3a).

There is direct evidence of winding of its ends around trajectory of particles emerging from disk side parts. Transverse projection presented in Fig. 3b shows nonlinear deformations in

vertical plane.

The method for calculation of vortex wake shape and induced velocities suggested in paper [1] includes thickness effect of diffused vortices. Thickness parameter of sheet of free vortex which start diffusing at $\varepsilon = 0.5\delta$ is taken in the form of

$$\varepsilon^2 = \varepsilon_0^2 + 4\nu_э(t-\tau), \qquad (1.4)$$

where $(t - \tau)$ is time of vortex life, ν_{ef}, is equivalent kinematic viscosity coefficient at turbulent diffusion in rotor vortex wake equal to

$$\nu_э = 0.0037 \cdot \left(\frac{\Gamma}{\nu}\right)^{\frac{3}{4}} \cdot \nu \approx 100\nu, \quad \text{where}$$

ν is ambient kinematic viscosity coefficient. The value of ε_0^2 is determined experimentally or computationally [1] based on
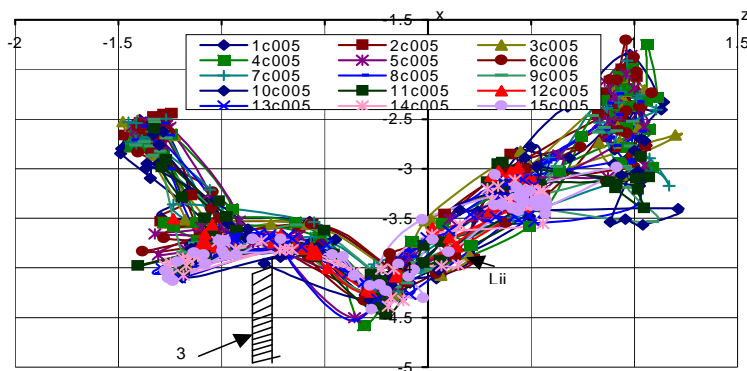
Figure 4: Arrangement of Li_j lines passing through each blade section with index j in the deformed "section", 3 – strip consisting of lateral vortex elements between points i and i+l

boundary layer thickness at the time of its separation from blade trailing edge. Vortex thickness ahead of Li_j curves and on them was determined by the expression (1.4). Behind these curves the rectilinear vortices generating the far vortex wake have the same value of vortex thickness parameter ε^2 as on curve Li_j. These values ranges from 0.0051 to 0.0055 at coefficient of turbulent viscosity in the wake $v_{ef}=0.005$ depending on radius and azimuth of calculated sections.

2. COMPUNANION OF INDUCED VELOCITIES

The problem of determining the induced velocities from free vortices at any point of space using the disk theory is reduced to the computation with subsequent summation of induced velocities caused by two types of vortices –the longitudinal and the lateral ones. Longitudinal vortices are integrated with respect to the inclined cylinder element.

Free lateral vortices are located in radial directions. Each elementary free lateral vortex is formed in rotor plane of rotation at the point with coordinates $\bar{\rho}_j$ and ψ when the lifting line goes through this point. Induced velocities are determined using semi-infinite vortex strip consisting of vortex elementary segments $d\vec{l}$. According to the disk theory it is equivalent to determination of induced velocity at the point (x,y,z) from vortex segment $d\vec{l}$ initiating at point (x_j, y_j, z_j) and ending at point (x_{j+1}, y_{j+1}, z_{j+1}) [4].

2.1 Computation of instantaneous induced velocities from semi-infinite vortices

Semi-infinite vortex field has no potential. In the present case semi-infinite vortices originate at points of termination of vortices determined by nonlinear theory (Figs. 3a,b and 5) and going to infinity in the direction of vortex cylinder drift velocity. Assume that semi-infinite vortex the circulation of which is known and constant along its entire length is given at its beginning at point on curve Li_j by radius-vector $\vec{r}_1$, Cartesian coordinates x_1, y_1, z_1. The direction of vortices is specified by a unit vector

$$\bar{l} = l_x\vec{i} + l_y\vec{j} + l_z\vec{k}, \text{ где } \quad |\bar{l}| = \sqrt{l_x^2 + l_y^2 + l_z^2} = 1, l_X = \cos(\alpha_c), l_Y = \sin(\alpha_c), l_Z = 0.$$

Computational points for determination of blade induced velocities from longitudinal vortices $\vec{w}_{np}$ are specified by radius-vector $\vec{r}$. Then the velocity at random point is calculated in vector expression using formulae [5]

$$\bar{\upsilon}_{np} = \frac{\Gamma}{2\pi}\bar{\upsilon}_\Gamma, \quad ,\bar{\upsilon}_\Gamma = \frac{(\vec{r} - \vec{r}_1) \times \bar{l}}{\left|(\vec{r} - \vec{r}_1) \times \bar{l}\right|^2}\left(1 + \frac{\bar{l} \cdot (\vec{r} - \vec{r}_1)}{|\vec{r} - \vec{r}_1|}\right) \cdot K(r), \qquad (2.1.1)$$

where $\overline{\Gamma}$ is a circulation of line vortex related to ωR^2.

As a result the induced velocities from vortex semi-infinite cylinder are defined as

$$\upsilon_{np_X} = \frac{\overline{\Gamma} \cdot k_L}{2\pi}\sum_1^{jv}\sum_0^{ip}\upsilon_{\Gamma_X}, \upsilon_{np_y} = \frac{\overline{\Gamma} \cdot k_L}{2\pi}\sum_1^{jv}\sum_0^{ip}\upsilon_{\Gamma_Y}, \upsilon_{np_z} = \frac{\overline{\Gamma} \cdot k_L}{2\pi}\sum_1^{jv}\sum_0^{ip}\upsilon_{\Gamma_Z}, \quad (2.1.2)$$

where ip is a number of azimuth dissections, jv is a number of radius dissections.

2.2 Induced velocities from vortex strip (line vortex segment of finite cross-section)

Velocity $d\bar{\upsilon}$ caused by infinitely thin vortex segment $d\vec{l}$ arbitrarily arranged in space is presented as

$$d\vec{\upsilon} = \frac{\Gamma}{4\pi} \cdot \frac{d\vec{l} \times \vec{r}}{\left[d\vec{l} \times \vec{r}\right]^2} \cdot \left(\frac{d\vec{l} \times \vec{r}_A}{r_A} - \frac{d\vec{l} \times \vec{r}_B}{r_B} \right) \cdot K(r).$$

The velocity caused by vortex of finite cross-section in view of the function K(r) will be

$$d\vec{\upsilon} = \frac{\Gamma}{4\pi} \cdot \frac{d\vec{l} \times \vec{r}}{\left[d\vec{l} \times \vec{r}\right]^2 + d\vec{l}^2 \varepsilon^2} \cdot \left(\frac{d\vec{l} \times \vec{l}_A}{\sqrt{l_A^2 + \varepsilon^2}} - \frac{d\vec{l} \times \vec{l}_B}{\sqrt{l_B^2 + \varepsilon^2}} \right) \times \vec{l}, \qquad (2.2.1)$$

Here, $\vec{l}_A$ and $\vec{l}_B$ are radius-vectors connecting the points A (coordinates x_1, y_1, z_1) and B (coordinates x_2, y_2, z_2) of the beginning and the end of vortex segment with velocity application point having coordinates x,y,z.

Finally, to calculate the induced velocities based on (2.11.2) and (2.2.2) we have of the whole system of far vortices (rectilinear vortex filaments for longitudinal vortices and rectilinear vortex strips for lateral vortices) the following relationships: for longitudinal component of induced velocity on x axis

$$\upsilon_x = \upsilon_{np_X} + \upsilon_{non_X} = \frac{\overline{\Gamma} \cdot k_L}{2\pi} \sum_1^{jv} \sum_0^{ip} \upsilon_{\Gamma_X} - \frac{\overline{\Gamma} \cdot k_L}{4\pi} \sum_1^{jv} \sum_0^{ip} \Delta\upsilon_x ,$$

axial component of induced velocity on y axis

$$\upsilon_y = \upsilon_{np_Y} + \upsilon_{non_Y} = \frac{\overline{\Gamma} \cdot k_L}{2\pi} \sum_1^{JV} \sum_0^{ip} \upsilon_{\Gamma_Y} - \frac{\overline{\Gamma} \cdot k_L}{4\pi} \sum_1^{jv} \sum_0^{ip} \Delta\upsilon_y ,$$

lateral component of induced velocity on z axis

$$\upsilon_z = \upsilon_{np_Z} + \upsilon_{non_Z} = \frac{\overline{\Gamma} \cdot k_L}{2\pi} \sum_1^{jv} \sum_0^{ip} \upsilon_{\Gamma_Z} - \frac{\overline{\Gamma} \cdot k_L}{4\pi} \sum_1^{jv} \sum_0^{ip} \Delta\upsilon_z .$$

3. COMPUTATIONAL RESULTS

The object of the present investigation is a helicopter rotor blade having a NACA 23010 airfoil over the entire span. The rotor lift coefficient in this case was equal to Ct=0.01074, the effective rotor angle of attack α_{ef}=0.85°, rotor cone angle α_0=1.146°. Flight conditions at $\mu = 0.0917$ were considered. Computations were made using nonlinear theory for rotor blade with the given circulation of shedding longitudinal and lateral vortices and with circulation defined from combined computation of rotor loads and the induction [1].

In Fig.5a and 6a in calculated section r/R =0.97 increments from far nonlinear wake of the induced velocities, determined when calculating the shortened 5-turn vortex sheet are presented. These increments were defined as

$$dV = V_{iy\partial} - V_{iy\kappa} \qquad (3.1)$$
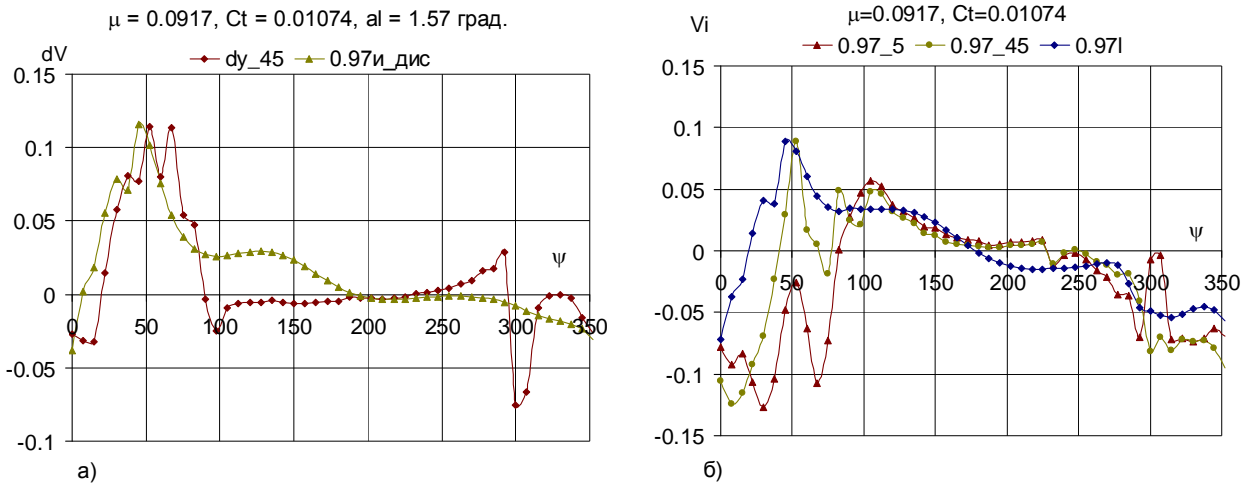
Figure 5: Induced velocities at the given vortex circulation in section r/R=0.97 : a) – additions from far nonlinear wake, "_45" –obtained from nonlinear calculation, "i-dis" – obtained by disk theory; b) –induced velocities "_5" – from shortened 5-turn wake, "_45" – from 45-turn wake, "l" – obtained using combined method

and they were rather noticeable (the second significant figure after a comma) for nonlinear wake.

Fig. 5a refers to the case when vortex circulation is given. The largest increments here are observed in the rear part of the swept disk at azimuths $\psi=0° - 90°$. In the plots the following symbols are introduced: dv_45 – for calculated increments according to (3.1) and _dis – for increments obtained by the disk theory from rectilinear vortices. Complete agreement between these two corrections to induced velocities caused by a shortened wake should not be expected. We can only say that the order of their magnitudes and the qualitative character of curves are the same. Also it should be noted that the effect of far wake is evaluated through the induced velocities from vortices of finite length although fairly substantial.

Similar computational results for distributions of circulation determined by combined computation with loads are shown in Fig. 6a.

In Fig. 5b the curves induced velocity are presented for the given circulation from vortices of 5-turn shortened wake (_5), from 45-turn wake (_45) and induced velocity from the entire vortex system obtained by the suggested combined method (1, see Fig. 3). The numerical results for complete induced velocities presented in Fig. 5b are obtained by summing up velocities from 5-turn shortened wake with additions from far wake determined by the disk theory. The induced velocities in all blade sections are qualitatively similar to other curves character. They illustrate that these induced velocities show more no disturbed character and their absolute values are lesser almost over the entire span. The results are presented only for the most loaded sections.
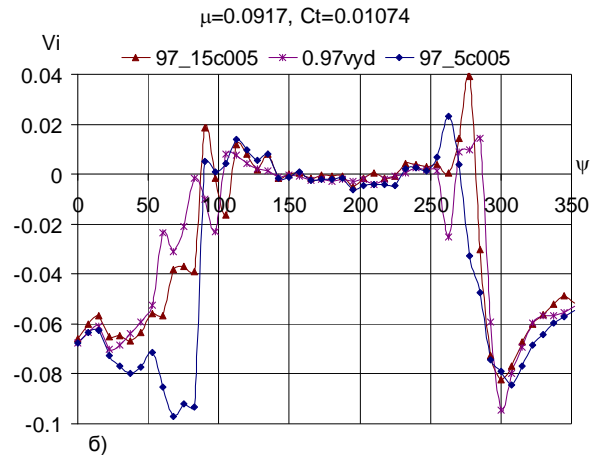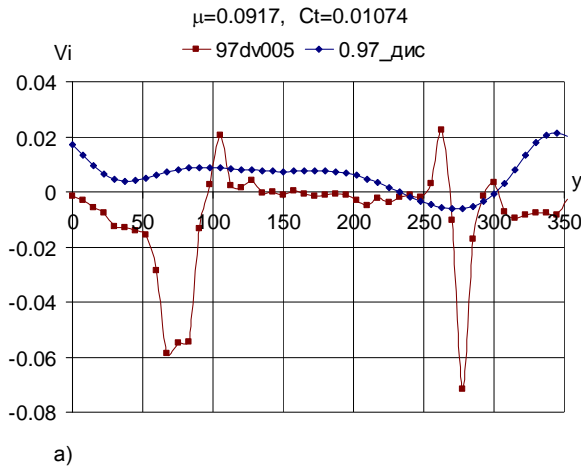
Figure 6: The same as in Fig. 5 , but the circulation of shedding vortices is determined in combination with induced velocities: a) – additions from nonlinear far wake, "dv005" – obtained from nonlinear calculation, "_dis" – obtained by disk theory: b) – induced velocities "_5c005" – from shortened 5-turn wake, "15c005" – from 15-turn wake, "vvd" – obtained using combined method

Computational results for vortex circulation distribution obtained from the combined computation of blade loads and induced velocities are presented in Fig. 6b. In this figure the symbol _5c005 denotes the induced velocity for the variant with shortened 5-turn wake and the symbol _15c005 means the same for 15-turn wake. The vyd curve illustrates the values of induced velocities obtained by summing up the induced velocities from nonlinear shortened vortex wake with the addition from far wake calculated by the disk theory. Apparent distinctions are observed in values of induced velocities in the rear part of the swept disk due to the influence of the far wake, especially in the first quarter at $\psi=0° – 90°$. The negative values of the induced velocities are smaller.

The values of instantaneous induced velocities from lateral far vortices are presented in Fig. 7.
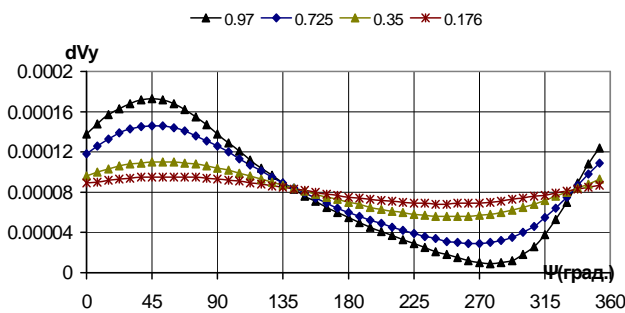
Figure 7: Additions to induced velocities from remote lateral vortices dvy over different blade sections

The absolute magnitudes of those values are too small (within the accuracy of computation) to have an effect on induced velocities in rotor plane and in rotor vortex wake.

Comparison of experimental and computational results is made for induced velocities in rotor vortex wake at $\psi= -45°$ (Fig. 8a and б) and at $\psi= 45°$ (Fig. 8в). The following symbols are introduced in these figures: the curve with symbol "exp"- for experimental average induced velocities, with symbol "_5c005"- for average induced velocities

from shortened wake and with symbol "vyd"- for average induced velocities in view of the effect of the far wake. In reference to quality the calculated induced velocities "vyd" represent the character of experimental induced velocities more exactly than that of velocities

from shortened vortex wake. In numerical expression "vyd" curves are also closer to experimental curves.

x/R = -0,79; z/R = 0б79, ψ=−45

x/R = -0,85; z/R = 0,85

x/R = -0,79; z/R = 0,79; ψ = 45

а)

б)

в)
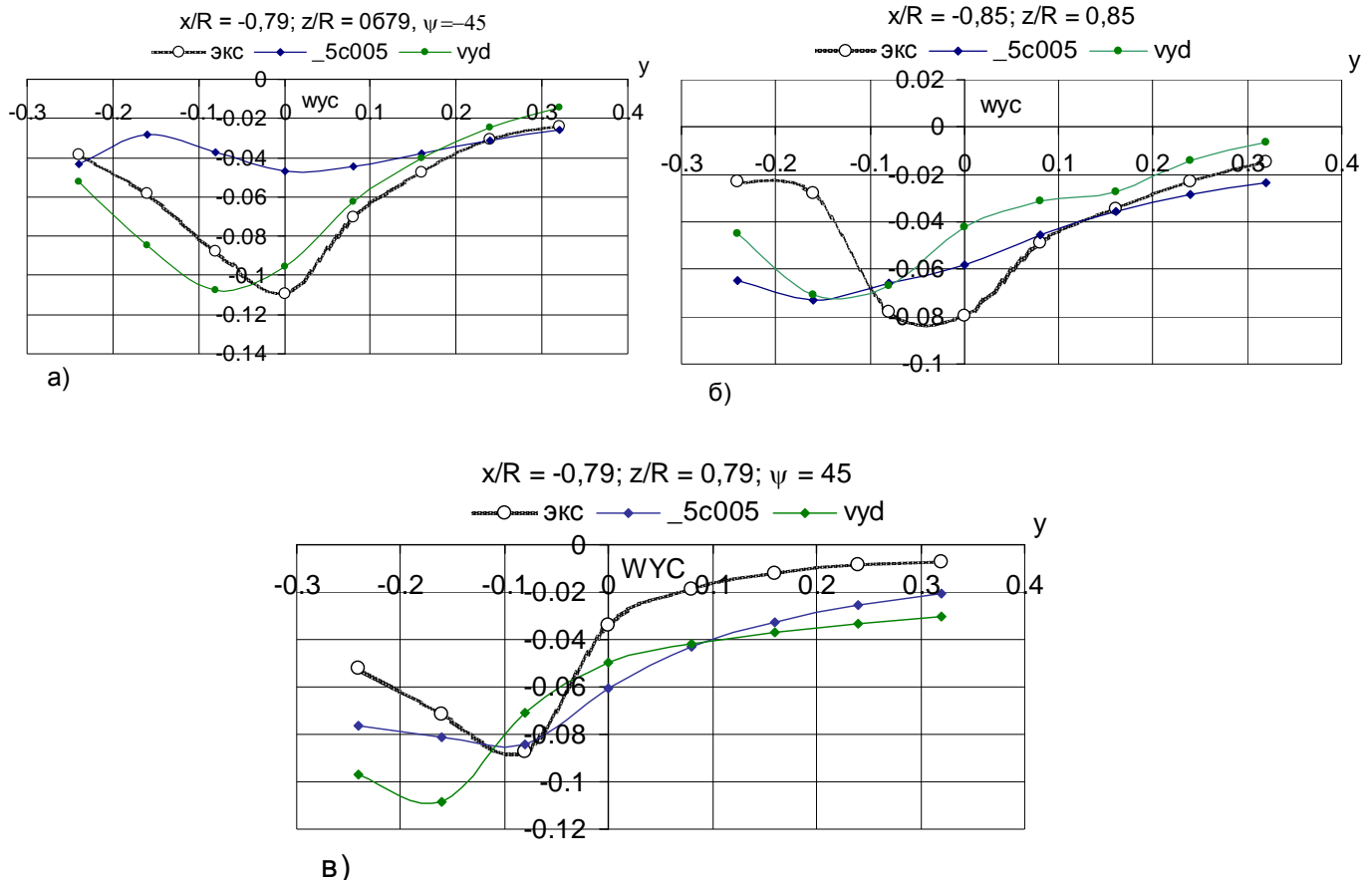
Figure 8: Comparison of average induced velocities at ψ= - 45° (a,b) and
ψ= 45° (c): experimental curves ("exp"), from shorted vortex 5-turn wake
(curve "_5c005"), in view of remote vortex wake (curve "vyd")

CONCLUSIONS

1 The conducted computations have shown that account of the far vortices at $\mu = 0.31$ at the given circulation has a little effect on induced velocities, if any, and has a little effect on induced velocities under circulation determined by the combined computation.

2 The effect of the far vortex wake at flight conditions $\mu = 0.0917$ is considerable for both the given circulation and the circulation determined from combined computation.

3 The proportion of induced velocities from far lateral vortices is extremely small in total induced velocities.

10

REFERENCES

[1] Shcheglova, V.M., "To the Computation of Rotor Induced Velocities in View of Vortex Diffusion by Nonlinear Model, Uchenye Zapiski TsAGI, 2007, Vol.XXXVIII, №3-4.

[2] Shcheglova, V.M., Mirgazov, R.M., "The Effect of Far Vortex Wake on Instantaneous Induced Velocity in Rotor Plane", FGUP "TsAGI", Materials of XVI School-Seminar "Aerodynamics of Flying Vehicles"- Zhukovsky, 2005, pp. 105-106.

[3] Baskin, V.E., Korolyova, K.K, "To the Nonlinear Vortex Theory of Helicopter Rotor in Horizontal Flight", Trudy TsAGI, 1966, issue 1013.

[4] Van Shi Zun',"Generalized Vortex Theory for Helicopter Rotor", the Problems of Helicopter Rotor Aerodynamics, MAI, M., Oborongiz, 1961, pp. 25-61.

[5] Babkin, V.I., Belotserkovsky, S.M., Gulyaev, V.V., Dvorak, A.V., "Jets and Lifting Surfaces", Modelirovanie na EVM, M., Nauka, 1989, p. 208.